



SEGMENTATION OF OCT IMAGE BY GRAPH CUT TECHNIQUE AND CLASSIFICATION BY SVM CLASSIFIER

Archanaa. S¹, Usha. A²

¹Department of ECE, Easwari Engineering College, (INDIA)

²Department of ECE, Easwari Engineering College, (INDIA)

ABSTRACT

Vision loss occurs mainly due to thickening or rupturing of blood vessels. The most common retinal disorder which prevail is cystoidal macular diabetic retinopathy. Diabetic retinopathy occurs due to increased blood sugar level in the body which leads to leakage of blood and other fluids leading to blurred vision or vision loss. The severity of this disease results in retinal detachment. The major issue in retinal disorder is detection of the abnormality at early stage which can help in early diagnosing of the disease. This paper uses a novel technique of detecting the abnormality automatically from the classification result obtained by means of SVM classifier. The accuracy attained varies in the range of 96%-98% in detection. This method provides an automatic detection of amount of abnormality which results in early detection of retinal disorder.

Keywords: *cystoidal macular diabetic retinopathy, Diabetic retinopathy, support vector machine(SVM)*

I. INTRODUCTION

It has been observed from analysis that about 80 million people around the world are affected due to low vision and other retinal disorders which may cause permanent loss of vision or low vision. The commonly occurring ocular disorder is mainly due to increase in blood sugar level which is known as diabetic retinopathy(DR) [4]. This at an initial stage leads to thickening of the retinal layers. Further it develops into leakage of blood and other retinal fluids into the retina causing blurred vision which is known as non-proliferative diabetic retinopathy(NPDR). In some severe cases, there exist blockage of blood vessels causing a deficiency towards blood supply. Hence, signals are sent by the region for nourishment. Due to the pathology, there is an abnormal growth of blood vessel into the vitreous chamber. These blood vessels are fragile, causing blood leakage and gradually leads to contraction of the vitreous chamber causing retinal detachment. This condition is known as proliferative diabetic retinopathy(PDR) [5] which may lead to blindness. For retinal disorders, the affected region is treated by means of laser light source or surgery in case of severity. To diagnose the disorder with lesser complexity early detection should be enabled. For proper diagnosis of the disorder, clear details of the retinal information are to be obtained. Optical coherence tomography [1], [2], [3] is a technique which provides micrometre resolution and axial cross section of images of translucent or opaque materials such as biological tissues using a low coherence light source.

OCT image acts as a guiding tool in diagnosing and by depending on the properties of the light source used the resolution varies. Fig 1.1 shows the OCT retinal image. The light source is focused at the center of the pupil which reaches the retinal region thereby producing the 3-dimensional view of the retinal layers with micro-resolution.

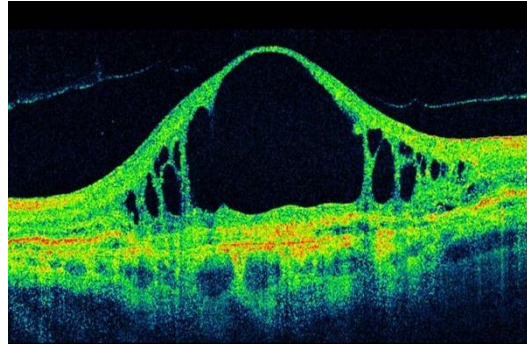


Fig 1.1 OCT Image of Affected Retina

OCT can be used for the early detection of DR since it has the ability to provide qualitative access of the retinal as well as pathological features and also make the quantitative measurements in an objective manner. In this paper, a semi-automatic technique for the classification of normal and abnormal image of retina is introduced. Generally, oct image is corrupted by means of speckle noise [1] which is denoised by using an efficient filter which is chosen on comparison with three other filters. It is important to enhance the pixels which contains the information of the data and so contrast enhancement is implemented. Then the image is segmented by using a novel technique called graph cut segmentation and k-means is used for clustering. The features are extracted from the clusters and then given to the classifier for classification process. Based on the number of true positives and false positives present in the image the classification is done which further gives the specificity and sensitivity of the concerned image.

II. METHODOLOGY

In overview, this method consists of the following flow: the image is denoised and enhanced in pre-processing. K-means algorithm is used for clustering process. The segmentation of foreground from background is done by means of graph cut technique which is shown in Fig 1.2. The RGB image is then converted to grey scaled image for simplicity and the features are extracted by using GLCM technique which are sent to the trained classifier which detects the normal and abnormal image.

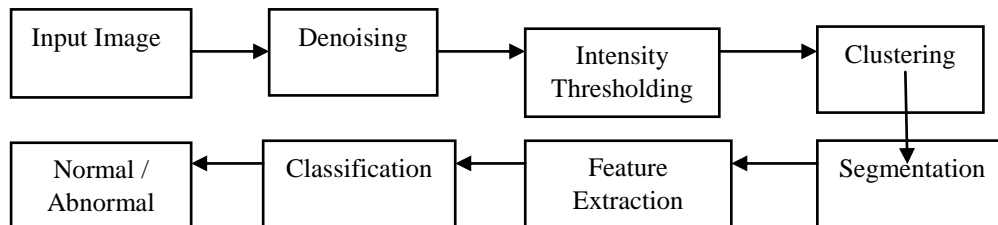


Fig 1.2 Block Diagram

1.1 Pre-Processing

Pre-processing is the primary stage of image processing. It involves improving the quality of the image without losing the data in the image and eliminates the uneven illumination present in the image and removes the noise present in the image. Here, speckle noise is present [6], [7], [8]. The input image is given to the filter which involves removal of noisy content present in it. For noise removal technique, an efficient filter is to be implemented. It has been found that anisotropic diffusion filter [6], [9], [10], [11] has good performance metric when compared to mean filter, adaptive bilateral filter and adaptive median filter. Smoothness of the image is directly proportional to the number of iterations. The smoothing operation is performed by

$$\frac{\partial I}{\partial t} = \text{div}(c(x,y,t)\nabla I) = \nabla c \cdot \nabla I + c(x,y,t)\Delta I \quad \dots(1)$$

Here Δ denotes the Laplacian, ∇ denotes the gradient and $c(x,y,t)$ is the divergence operator and is the diffusion coefficient. $c(x,y,t)$ controls the rate of diffusion and is usually chosen as a function of the image gradient so as to preserve edges in the image. Fig 1.3 shows the pre-processed image.

1.2 Image Enhancement

The pixels which contains the information should be highlighted in order to obtain the clear details of the image. Here we use intensity thresholding to enhance the important pixels. This is implemented by setting a threshold value. The pixels which are within the threshold range is highlighted and the remaining pixels below and above the range are eliminated thus giving an enhanced image. Fig 1.4 shows the enhanced image in which contrast stretching occurs.

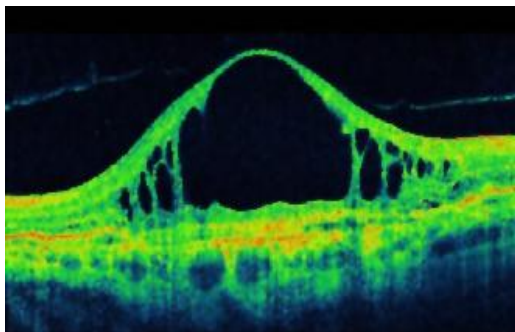


Fig 1.3 Anisotropic Diffusion Filter Output

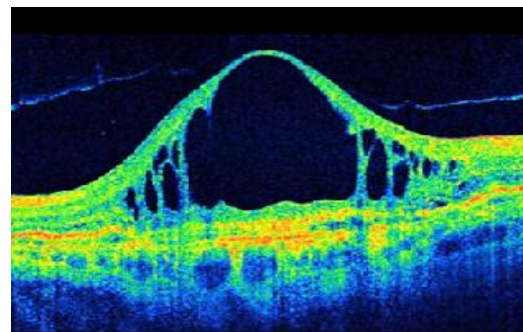


Fig 1.4 Contrast Enhanced Image with Intensity Thresholding

1.3 Clustering

Clustering is the process of grouping up of pixels. This paper utilizes k-means clustering algorithm [12], [13] which forms distinct k-clusters from a given data points. It mainly involves calculation of k-centroid and taking each point from a data set to the cluster which has the nearest centroid. Initially it involves determining the number of k-clusters and centroid pixels. Then the Euclidean distance between each pixel and the center is calculated by the relation,

$$d = \| p(x,y) - C_k \| \quad \dots(2)$$

where d is the Euclidean distance and C_k is the cluster centers of the input pixels $p(x,y)$ which are to be clustered. The pixels are assigned to the nearest center pixel based on the distance and then the new position of the center pixel is calculated using the relation,

$$C_k = \frac{1}{k} \sum_{y \in C_k} \sum_{x \in C_k} p(x, y) \quad \dots (3)$$

This process is repeated until the tolerance or error value is satisfied. In this paper, clusters are formed based on the pixel intensity and hence three clusters are formed as shown in Fig 1.5. The center pixel is first assigned and then the value of the pixel is replaced by the average of the neighbourhood pixels. The cluster which has good features is then given to the classifier as input.

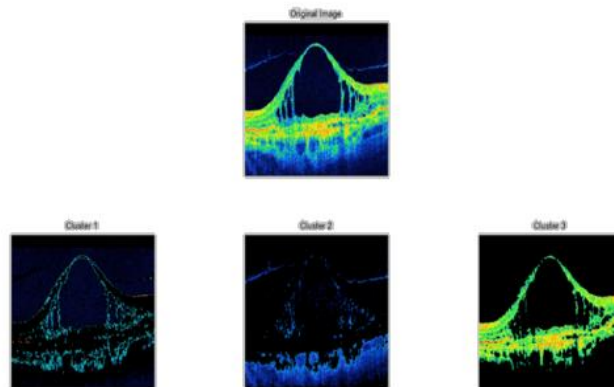


Fig 1.5 Clusters of the given Image

1.4 GRAPH CUT SEGMENTATION

In order to focus of the retinal layers, it is essential to separate the foreground image from the background image. In general, Graph cut segmentation [11], [15] is a novel technique for segmentation of images. In this technique, the graph [14] is framed by means of assigning nodes where the pixels in the region are taken as nodes. The RGB image is converted to grey image so that only two values exist namely 0 and 1. Two nodes are assigned at the front and back of the nodes as source and sink nodes. The source node concentrates on the nodes which have the value of 0 i.e., foreground and the sink node focuses on the nodes with value 1 i.e., background. This enables the formation of min-cut which separates the foreground and background of the image as shown in Fig 1.6. Here the segmentation is done based on the intensity of the pixels. For simplification, it is assumed that the mean intensity μ_1 of the region of interest is known along with that of the background's μ_0 and the computation the energy function $E(\Omega)$ is minimized.

$$E(\Omega) = \lambda \cdot \text{length}(\partial\Omega) + \sum (I(x_i) - \mu_0)^2 + \sum (I(x_i) - \mu_1)^2 \quad \dots (4)$$

Here the edges of the pixels at the foreground are connected to the source and a weight is set as $(I(x_i) - \mu_1)^2$. Similarly, the edges of the pixel at the background are connected to the sink with weight $(I(x_i) - \mu_0)^2$. The weights between the center pixel and its neighbourhood pixel always equals the value of Y for all the edges. The Y with low value denotes the data and Y with high value denotes the boundary. From these values the min-cut of the graph can be computed and segmentation is performed. On segmenting the foreground image from background the abnormality can be analysed with less complexity.

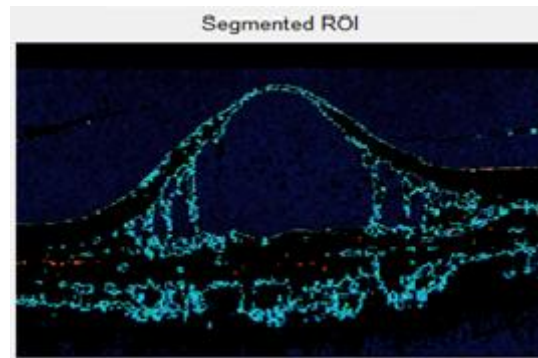


Fig 1.6 Segmented Image with region of interest

1.5 Feature Extraction

Feature extraction is the process of retrieving the important data from a given raw data. The set of parameters found is used to define the shape of a character in a precise and unique manner. In this phase, the character is represented by a feature vector [17] which becomes its identity. The RGB image is converted to grey image to reduce the complexity level. Then the texture feature of the image is obtained. Generally, the texture feature [16] is classified as first order and second order features. The first order features rely on a single pixel and not on the relation with neighbourhood pixels. Mean, variance, skew and kurtosis histogram features of first order. Second order features gives the relation between the pixel and its neighbourhood pixels. Texture features are extracted by means of using GLCM technique.

1.5.1 GLCM

Gray-level co-occurrence matrix (GLCM) [18], [19], [20] describes the spatial relationship between each intensity tone. The first step in GLCM is computation of co-occurrence matrix followed by calculation of texture features based on the matrix. In transformation process, the relationship between the neighbourhood pixels is represented as co-occurrence spaces in the matrix and the neighbouring pixels in the direction 0° , 45° , 90° , 135° and its reverse direction since it has the position of the pixels with same gray level. The number of times pixel with value i occurs adjacent to the pixel with value j , it is specified by an element $P(i,j)$ in GLCM [23]. Consider an image of size $N \times N$, then the co-occurrence matrix is framed by

$$P(i, j) = \sum_{x=1}^N \sum_{y=1}^N \begin{cases} 1; & I(x, y) = i \text{ and } I(x + \Delta x + \Delta y) = j \\ 0; & \text{otherwise} \end{cases} \dots(5)$$

Δx and Δy is the offset which denotes the distance between the center pixel and its neighbourhood pixels. Let i and j be the co-efficient of the co-occurrence matrix and $p(i, j)$ the element of the matrix.

II. CLASSIFICATION

Classification is the process of differentiating the normal image from abnormal image. The classification process depends mainly on the features obtained from the image. By enabling an efficient classifier, the sensitivity and specificity of the given image can be improved. Classification involves training and testing set. In training set, each class label has several features. In this paper, SVM classifier [20], [21], [22] is used for the classification process. SVM [23] usually consists of a hyperplane which is used to distinguish the data sets.

Based on the operation it is classified as linear and non-linear. If the data from different classes can be separated, the classifier is said to be linear else non-linear. The linear classifier is represented as

$$f(x) = w^T x + b \quad \dots (6)$$

Similarly, the non-linear classifier is represented as

$$f(x) = w^T \phi(x) + b \quad \dots (7)$$

Here, w represents the weight of the vector and b is the threshold and x_i is the data point. By using kernel the non-linear data is transformed to linear data in high dimension. In order to improve the efficiency, multi-SVM is implemented. Multi-SVM is constructed by combining individual SVM in a one-against-all fashion or many-against-one fashion. It performs classification of both linear and non-linear data which makes it more compatible. The multi-SVM is represented by

$$f(x) = k \sum_{m=1}^k w_m^T \phi(x) + b \quad \dots (8)$$

where k is the number of classes and m is the m^{th} SVM used for classification.

III. RESULTS AND DISCUSSIONS

In this paper, the comparison has been done between the parameters of 2D median, adaptive bilateral, anisotropic diffusion and adaptive median filter. It is found that anisotropic diffusion filter has good performance for OCT images. The parameters of the filters for processing a single OCT image is shown in Table I.

TABLE I: Parameters of The Filters

Filters	PSNR	MSE	MEAN	SNR
Median	19	28.95	45.67	28.59
AMF	34	27.25	43.98	36.25
ADF	35.5	30	46.33	38.66
ABF	34	37.66	46.09	38.008

For improving the characteristic of the image, parameters of the image are calculated which is shown in Table II. AMBE, SSIM and CWSSIM factors decide the image quality and enables to figure out even the small pixels of the image i.e., the small distortions in image can also be eliminated. AMBE is used to find the closeness of prediction to the evaluated outcomes.

$$AMBE = E(y) - E(x) \quad \dots (9)$$

where $E(y)$ is the output mean and $E(x)$ is the input mean of the image. Similarly, the CWSSIM (C_w) and SSIM of the image are found by using the formula (10) and (11)

$$C_w = \frac{(I_f - I_b)}{I_b} \quad \dots (10)$$

Here, I_f and I_b are the minimal and maximal intensities of the foreground and background image.

$$SSIM(x,y) = \frac{(2\mu_x \mu_y + C_1)(2\sigma_{x,y} + C_2)}{(\mu_x^2 + \mu_y^2 + C_1)(\sigma_x^2 + \sigma_y^2 + C_2)} \quad \dots (11)$$

where μ_x is the average of x , μ_y is the average of y , σ_x is the variance of x , σ_y is the variance of y , $\sigma_{(x,y)}$ is the co-variance of x and y and C_1 and C_2 are the variables to stabilize the division with weak denominator.

TABLE II: Parameters of Oct Image

NUMBER OF IMAGES	AMBE	SSIM	CWSSIM
1	36.057	0.0687	0.1280
2	28.85	0.0714	0.1339
3	35.89	0.0725	0.1336
4	29.78	0.0135	0.6357
5	35.89	0.132	0.2182
6	15.91	0.0312	0.6446
7	11.65	0.0135	0.6357

Feature extraction involves reducing the amount of resources required to describe a large set of data i.e., maximizing the recognition rate with limited number of elements. In this paper, the features extracted are shown in Fig.1.4 for a single abnormal image and for dataset in Table III.

TABLE III: FEATURES EXTRACTED FOR A DATASET OF ABNORMAL IMAGE

Features	Image 1	Image 2	Image 3	Image 4	Image 5	Image 6
Mean	16.27	15.53	21.94	15.66	18.16	14.42
Variance	1675	1410	1770	1554	2078	1339.6
Energy	0.697	0.689	0.307	0.699	0.377	0.684
Entropy	3.416	3.40	3.48	3.37	2.31	3.20
Contrast	1.218	1.086	0.662	1.187	0.605	0.857
Correlation	0.494	0.461	0.374	0.473	0.396	0.352
Smoothness	1	1	1	1	1	1
IDM	255	255	255	255	255	255
Skew	3.789	3.97	2.53	3.94	2.92	4.06
Kurtosis	17.74	19.97	9.40	19.25	11.97	20.60
SD	41.57	38.27	46.5	40.06	47.15	38.08
Homogeneity	0.905	0.903	0.812	0.906	0.835	0.902

The features are sent to the classifier where the sensitivity and specificity of the image is obtained. The sensitivity (S_N) of the image is the ability to identify the positive result. It is obtained by calculating the number of true positives (x_T) and number of false negatives (y_N).

$$S_N = \frac{x_T}{(x_T + y_N)} \quad \dots (12)$$

Term specificity is the ability to identify the negative result and is obtained by calculating the number of true negative (x_N) and the number of false positives(y_P).

$$S_P = \frac{x_N}{x_N + y_P} \quad \dots (13)$$

Depending on the sensitivity and specificity the accuracy is calculated. The affected region is estimated by using

$$A = \frac{A_1 \cdot a}{A_2 \cdot a} \quad \dots (14)$$

where A_1 is the detected region, A_2 is the affected region and a is the area. The overview of the process is shown in Fig 1.7

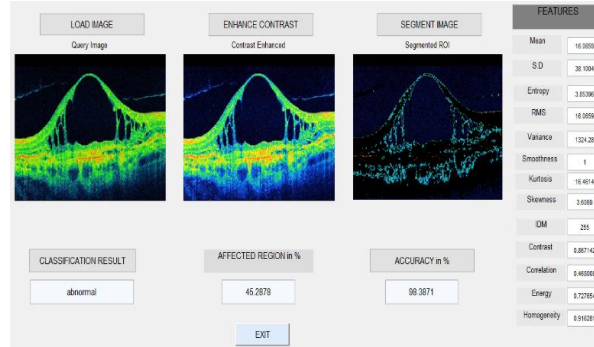


Fig 1.7 Classification and Detection of Abnormality

IV CONCLUSION

Detection of retinal disorders at an early stage with high accuracy is a challenging process. In this paper, a comparatively good filter for the removal of speckle noise and a novel technique to detect the ocular disorder at an early stage is implemented. This process is enabled by means of segmenting the image by graph cut technique [15] and by using SVM and Multi-SVM classifier [22] and [24] which takes features extracted as the input. In addition, more focus is given to accuracy which is determined by the sensitivity and specificity [25] obtained from the image. This paper iteration value of 500 is used for accuracy, the larger the number of iterations the greater is the accuracy. Results showed that the accuracy attained is about 96%-98%. In the computation process, the increase in number of iterations increases the computation time. Hence, more concentration should be given in reduction of computation time without decreasing the true positives.

REFERENCE

- [1] D. Huang, E. A. Swanson, C. P. Lin, J. S.Schumann, W. G. Stinson, M. Chang, M. R. Hee, T. Flotte, K. Gregory, C. A. Puliafito, and J. G. Fujimoto, "Optical coherence tomography," vol. 254, JULY 1991.
- [2] Jinming Duan, Christopher Tenchy, Irene Gottlobz, Frank Proudlockz, Li Bai "Optical Coherence Tomography Image Segmentation," vol.24, DECEMBER 2015
- [3] Gary R. Wilkins, Odette M. Houghton, and Amy L. Oldenburg, "Automated Segmentation of Intraretinal Cystoid Fluid in Optical Coherence Tomography," vol. 59, APRIL 2012.
- [4] Jathurong Sugruk, Supaporn Kiattisin and Adisorn Leelasantitham, "Automated Classification between Age-related Macular Degeneration and Diabetic Macular Edema in OCT Image Using Image Segmentation," vol.14, JULY 2014.
- [5] Archana.D.N, Padmasini.N, Mohamad Yacin.S, Umamaheshwari.R, "Detection of Abnormal Blood Vessels in Diabetic Retinopathy Based on Brightness Variations in SDOCT Retinal Images," vol.15, MARCH 2015.
- [6] Padmasini.N, Mohamad Yacin.S, Umamaheshwari.R, "Speckle Noise Reduction In Spectral Domain Optical Coherence Tomography Retinal Images Using Anisotropic Diffusion filtering," vol.14, APRIL 2014.



- [7] J. M. Schmitt, S. H. Xiang, and K. M. Yung, "Speckle in optical coherence tomography," vol. 4, JANUARY 1999.
- [8] Kirk W. Gossage, Tomasz S. Tkaczyk, Jeffrey J. Rodriguez, Jennifer K. Barton "Texture analysis of optical coherence tomography images: feasibility for tissue classification," vol.8, JULY 2003
- [9] Rupsa Datta, S Aditya, D N Tibrewala, "Advancement in OCT and image-processing techniques for automated ophthalmic diagnosis," vol.4, APRIL 2010.
- [10] Florence Rossant, Itebeddine Ghorbel, Isabelle Bloch, Michel Paques, Sarah Tick "Automated Segmentation Of Retinal Layers In Oct Imaging And Derived Ophthalmic Measures," vol.28, AUGUST 2009
- [11] Xiayu Xu, Kyungmoo Lee, Li Zhang, Milan Sonka, and Michael D. Abràmoff "Stratified Sampling Voxel Classification for Segmentation of Intraretinal and Subretinal Fluid in Longitudinal Clinical OCT Data," vol. 34, JULY 2015
- [12] Nameirakpam Dhanachandra, Khumanthem Manglem and Yambem Jina Chanu "Image Segmentation using K-means Clustering Algorithm and Subtractive Clustering Algorithm," vol.54, MARCH 2015
- [13] Weiguang Ding, Mei Young, Serge Bourgault, Sieun Lee, David A. Albani, Andrew W. Kirker, Farzin Forooghian, Marinko V. Sarunic, Andrew B. Merkur, and Mirza Faisal Beg "Automatic Detection of Subretinal Fluid and Sub-Retinal Pigment Epithelium Fluid in Optical Coherence Tomography Images," vol.3, JULY 2013
- [14] Kyungmoo Lee, Meindert Niemeijer, Mona K. Garvin, Member, Young H. Kwon, Milan Sonka, Fellow and Michael D. Abràmoff, "Segmentation of the Optic Disc in 3-D OCT Scans of the Optic Nerve Head," vol. 29, JANUARY 2010
- [15] Yuri Boykov, Gareth Funka-Lea, "Graph Cuts and Efficient N-D Image Segmentation," vol.15, JUNE 2006
- [16] Gaurav Kumar, Pradeep Kumar Bhatia, "A Detailed Review of Feature Extraction in Image Processing Systems," vol.74, FEBRUARY 2014
- [17] Muhammad Arif Mohamad, Dewi Nasien, Haswadi Hassan, Habibollah Haron "A Review on Feature Extraction and Feature Selection for Handwritten Character Recognition," vol. 6, APRIL 2015
- [18] A. Gonzalez, B. Remeseiro, M. Ortega, M.G.Penedo, "Automatic Cyst Detection in OCT Retinal Images Combining Region Flooding and Texture Analysis," vol.10, OCTOBER 2013
- [19] Shrikant D. Kale, Krushil M. Punwatkar, "Texture Analysis of Ultrasound Medical Images for Diagnosis of Thyroid Nodule Using Support Vector Machine," vol. 2, OCTOBER 2013
- [20] N. Anantrasirichai, Alin Achim, James E Morgan y, Irina Erchovay, Lindsay Nicholson, "SVM-Based Texture Classification In Optical Coherence Tomography," 2013
- [21] Gauri Borkhade, Dr. Ranjana Raut, "Support Vector Machine Neural Network Based Optimal Binary Classifier for Diabetic Retinopathy," vol. 3, JANUARY 2015
- [22] Abhishek Dey and Samir K. Bandyopadhyay "Automated Glaucoma Detection Using Support Vector Machine Classification Method," vol.12, OCTOBER 2015
- [23] Anuradha.K, Dr. K. Sankaranarayanan, "Statistical Feature Extraction To Classify Oral Cancers," Vol.4, FEBRUARY 2013



- [24] Chih-Wei Hsu and Chih-Jen Lin, “A Comparison of Methods for Multi-class Support Vector Machines,” vol.13, DECEMBER 2002
- [25] B. Vinothkumar, R. Harikumar “Performance Analysis of Em, SVD and SVM classifiers in classification of Carcinogenic Regions of Medical Images,” vol.43, JANUARY 2014